

# A family of mimetic finite difference methods on polygonal and polyhedral meshes

Franco Brezzi\*    Konstantin Lipnikov<sup>†‡</sup>    Valeria Simoncini<sup>§</sup>

March 17, 2005

## Abstract

A family of inexpensive discretization schemes for diffusion problems on unstructured polygonal and polyhedral meshes is introduced. The material properties are described by a full tensor. The theoretical results are confirmed with numerical experiments.

## 1 Introduction

In many applications, the mathematical model is formulated initially as a system of first order partial differential equations, with each equation having a natural connection to physical aspects of the problem. Thus, the increasing demand for accurate and robust numerical simulations has generated considerable interest in discretizations of this first-order form.

In this paper, we consider the diffusion problem written as a system of two equations:

$$\operatorname{div} \vec{F} = b, \quad \vec{F} = -\mathbb{K} \operatorname{grad} p \quad (1.1)$$

where the first equation describes the mass conservation and the second one is the constitutive equation relating the scalar function  $p$  to the velocity field  $\vec{F}$ . The material properties are described by  $\mathbb{K}$  which is generally a full symmetric tensor. The mimetic finite difference (MFD) method has been successfully employed for solving this problem on simplicial [13], quadrilateral [9, 11], hexahedral [14], and unstructured polygonal [10] and polyhedral [12] meshes in both Cartesian and cylindrical [15] coordinate systems.

Unstructured polygonal and polyhedral meshes appear, for instance, in geoscience problems simulating the flow and transport in porous media and using dual or median meshes.

---

\*Università di Pavia, Department of Mathematics, Pavia, Italy, [brezzi@imati.cnr.it](mailto:brezzi@imati.cnr.it)

<sup>†</sup>Los Alamos National Laboratory, Theoretical Division, MS B284, Los Alamos, NM, 87545, [lipnikov@lanl.gov](mailto:lipnikov@lanl.gov)

<sup>‡</sup>Corresponding author

<sup>§</sup>Dipartimento di Matematica, Università di Bologna, Piazza di Porta S. Donato, 5, I-40127 Bologna, Italy; IMATI-CNR, Pavia and CIRSA, Ravenna, Italy ([valeria@dm.unibo.it](mailto:valeria@dm.unibo.it)).

Adaptive locally refined meshes, non-matching meshes, hybrid meshes with complex transition regions filled with polyhedral elements are also examples of polyhedral meshes with degenerate and non-convex elements. The discretization methodology developed in [10, 4] allows to treat all these meshes within a single framework.

The key element of the MFD method is the scalar product in the space of discrete velocities which should satisfy the stability assumption **(S1)** and the consistency assumption **(S2)**(see below (3.2) and (3.3)). It turns out that such a scalar product is not unique. In the case of triangular meshes, we get a one-parameter family of acceptable scalar products and thus a one-parameter family of the corresponding discretization schemes [13]. One of these discretization schemes is the mixed finite element method with the lowest order Raviart-Thomas elements. Unfortunately, the algorithms developed in [13] are extremely difficult to extend even to quadrilateral meshes. In this paper, we employ an innovative technique to give a rigorous mathematical description of *a family* of acceptable scalar products for very general meshes in two and three dimensions. This generates a family of corresponding mimetic discretizations with similar properties. We prove that the dimension of this family grows quadratically with the number of edges for polygonal elements in 2D and with the number of faces for polyhedral elements in 3D.

The existence of a family of mimetic discretizations can be used to attack a number of computational problems. For instance, we may search this family for a scheme which satisfies some additional properties, as for instance the discrete maximum principle.

The convergence of mimetic discretizations has been analyzed in [4]. In the present paper we use the same set of assumptions used there, and therefore the theoretical results obtained in [4] hold for the discrete schemes derived here.

The discretization method developed in this paper is computationally *much cheaper and easier to implement* than the method described in [10, 12]. The optimal implementations of both methods result in complexity estimates that differ at least for one order of magnitude. In addition to that, the method from [10, 12] requires a partition of a mesh element into simplicial elements which is a non-trivial task for a non-convex element.

The outline of the paper is as follows. In Section 2, we describe briefly the mimetic finite difference method and formulate two sufficient conditions for the scalar product in the space of discrete velocities. In Section 3, we prove that there exists a family of acceptable scalar products, and we show how to construct them in practice. In Section 4, we confirm our theoretical results with numerical experiments on polygonal and polyhedral meshes.

## 2 A mimetic finite difference method

To simplify the presentation, we consider the homogeneous Dirichlet boundary value problem. Other types of boundary conditions are naturally embedded in the mimetic methodology [8].

Let  $\Omega \in \mathfrak{R}^d$  be a polygon ( $d = 2$ ) or a polyhedron ( $d = 3$ ) with a Lipschitz continuous boundary. Furthermore, let  $\Omega_h$  be a non-overlapping conformal partition of  $\Omega$  into simply-connected polygonal or polyhedral elements with flat faces. To use the convergence estimates proved in [4], we need some basic assumptions of shape regularity formulated there. Since these assumptions are not required until Section 3, we discuss them later.

Just to simplify the presentation, we assume that the tensor  $\mathbb{K}$  is constant inside each mesh element but may strongly vary across mesh faces (edges in 2D). We also assume that  $\mathbb{K}$  is strongly elliptic that is there exist two positive constants  $\kappa_*$  and  $\kappa^*$  such that

$$\kappa_* \|\mathbf{v}\|^2 \leq \|\mathbb{K}^{1/2} \mathbf{v}\|^2 \leq \kappa^* \|\mathbf{v}\|^2 \quad \forall \mathbf{v} \in \mathfrak{R}^d. \quad (2.1)$$

The *first* step of the MFD method is to specify the degrees of freedom for the primary variables  $p$  and  $\vec{F}$  which we shall refer to as the pressure and the flux, respectively. We consider the space  $Q^h$  of discrete pressures that are constant on each element  $E$ . For  $\mathbf{q} \in Q^h$ , we denote by  $q_E$  its value on  $E$ . The number,  $N_Q$ , of discrete pressure unknowns is equal to the number of mesh elements.

The space  $X^h$  of discrete velocities is defined as follows. To every element  $E$  and to every face (edge in 2D)  $e$  of  $E$ , we associate a number  $F_E^e$  and the vector field  $F_E^e \vec{n}_E^e$  where  $\vec{n}_E^e$  is the unit outward normal to  $e$ . We clearly make the continuity assumption

$$F_{E_1}^e = -F_{E_2}^e \quad (2.2)$$

for each face  $e$  shared by two elements  $E_1$  and  $E_2$ . The number,  $N_X$ , of discrete velocity unknowns is then equal to the number of boundary faces plus twice the number of internal faces. It is convenient to consider the space  $X^h$  as the subspace of  $\mathfrak{R}^{N_X}$  that verifies (2.2).

The *second* step of the MFD method is to define suitable scalar products in the discrete spaces. In the space  $Q^h$ , the scalar product is almost straightforward:

$$[\mathbf{p}, \mathbf{q}]_{Q^h} = \sum_{E \in \Omega_h} p_E q_E |E|, \quad (2.3)$$

where  $|E|$  is the volume (area in 2D) of  $E$ . In the space  $X^h$ , the scalar product is defined as follows:

$$[\mathbf{F}, \mathbf{G}]_{X^h} = \sum_{E \in \Omega_h} [\mathbf{F}, \mathbf{G}]_E \quad (2.4)$$

where  $[\mathbf{F}, \mathbf{G}]_E$  is a scalar product on the element  $E$ . Let  $e_1, e_2, \dots, e_{k_E}$  be a numbering of the faces of the element  $E$  (where  $k_E$  is clearly the total number of faces). The definition of the scalar product implies that there exists a symmetric positive definite  $k_E \times k_E$  matrix  $\mathbb{M}_E$  ( $\mathbb{M}_E = \mathbb{M}_E^T > 0$ ) such that

$$[\mathbf{F}, \mathbf{G}]_E = \sum_{s,r=1}^{k_E} \mathbb{M}_{E,s,r} F_E^{e_s} G_E^{e_r}. \quad (2.5)$$

Here and in the sequel,  $\mathbb{M}_{s,r}$  indicates the  $(s, r)$  entry of the given matrix  $\mathbb{M}$ .

Some minimal approximation properties for the scalar product (2.5) are required, that make the construction of the matrix  $\mathbb{M}_E$  a non-trivial task. It was shown in [4] that two conditions on (2.5) are sufficient for the convergence of the MFD method. We formulate and analyze these conditions in the next section.

The *third* step of the MFD method is to discretize the divergence operator. For each  $\mathbf{G}$  in  $X^h$  we define  $\mathcal{DIV}^h \mathbf{G}$  as the element of  $Q^h$  defined, in each element  $E$ , by

$$(\mathcal{DIV}^h \mathbf{G})_E := \frac{1}{|E|} \sum_{i=1}^{k_E} G_E^{e_i} |e_i|, \quad (2.6)$$

where  $|e_i|$  is the area (length in 2D) of the face  $e_i$ . Note that (2.6) is in perfect agreement with the Gauss divergence theorem.

The *fourth* step of the MFD method is to define the discrete flux operator,  $\mathcal{G}^h$ , as the adjoint to the discrete divergence operator,  $\mathcal{DIV}^h$ , with respect to scalar products (2.3) and (2.4), i.e.

$$[\mathbf{F}, \mathcal{G}^h \mathbf{p}]_{X^h} = [\mathbf{p}, \mathcal{DIV}^h \mathbf{F}]_{Q^h} \quad \forall \mathbf{p} \in Q^h \quad \forall \mathbf{F} \in X^h. \quad (2.7)$$

Using the discrete flux and divergence operators, the continuum problem (1.1) is discretized as follows:

$$\mathcal{DIV}^h \mathbf{F}_h = \mathbf{b}, \quad \mathbf{F}_h = \mathcal{G}^h \mathbf{p}_h \quad (2.8)$$

where  $\mathbf{b}$  is the vector of mean values of the source function  $b$ .

It was mentioned in many papers that the scalar product (2.5) in the MFD method is not unique. Different scalar products result in different MFD methods. In the next section we present the first rigorous mathematical description of a family of convergent MFD methods on unstructured polygonal and polyhedral meshes.

### 3 A family of accurate scalar products

Let us define an interpolation operator from the space of smooth enough vector-valued functions to the discrete space  $X^h$ . For every  $\vec{G} \in (L^s(\Omega))^3$ ,  $s > 2$ , with  $\text{div } \vec{G} \in L^2(\Omega)$ , we define  $\mathbf{G}^I \in X^d$  by

$$(\mathbf{G}^I)_E^e := \frac{1}{|e|} \int_e \vec{G} \cdot \vec{n}_E^e \, d\Sigma \quad \forall E \in \Omega_h \quad \forall e \in \partial E. \quad (3.1)$$

Following [4], we begin our analysis with the following two conditions for the scalar product (2.5).

**(S1)** There exist two positive constants  $s_*$  and  $S^*$  such that for every element  $E$  in the decomposition we have

$$s_* \sum_{s=1}^{k_E} |E| (G_E^{e_s})^2 \leq [\mathbf{G}, \mathbf{G}]_E \leq S^* \sum_{s=1}^{k_E} |E| (G_E^{e_s})^2 \quad \forall \mathbf{G} \in X^h. \quad (3.2)$$

**(S2)** For every element  $E$ , every linear function  $q^1$  on  $E$  and every  $\mathbf{G} \in X^h$ , we have

$$[(\mathbb{K} \nabla q^1)^I, \mathbf{G}]_E + \int_E q^1 (\mathcal{DIV}^h \mathbf{G})_E \, dV = \sum_{s=1}^{k_E} G_E^{e_s} \int_{e_s} q^1 \, d\Sigma. \quad (3.3)$$

Assumption **(S1)** states that matrix  $\mathbb{M}_E$  is spectrally equivalent to the scalar matrix  $|E| \mathbb{I}_d$  where  $\mathbb{I}_d$  is the identity matrix. In practice, the constants  $s_*$  and  $S^*$  are expected to depend only on the skewness of mesh elements and on the tensor  $\mathbb{K}$ . Assumption **(S2)** is the Gauss-Green formula with the constant velocity  $\mathbb{K} \nabla q^1$ .

Since the divergence of  $\mathbf{G}$  is a constant, the second term in (3.3) can be easily computed. Thus, this assumption results in a system of linear equations where the unknowns are the

coefficients of matrix  $\mathbb{M}_E$ . It was shown in [4] that this system has a solution. In the rest of this section, we present a new method for finding a family of matrices  $\mathbb{M}_E$  satisfying (3.2) and (3.3).

Taking  $q^1 = 1$  in (3.3), we get the formula for the discrete divergence operator. As we obviously expect frame invariance, we use this freedom and, for every element  $E$ , we set the origin in the center of mass of  $E$  which simplifies the construction of the matrix  $\mathbb{M}_E$ . Thus, Assumption **(S2)** can be replaced by the following one.

**(S2')** For every element  $E$  with center of mass at the origin and every  $\mathbf{G} \in X^h$ , we have

$$[(\mathbb{K}\nabla x_i)^T, \mathbf{G}]_E = \sum_{s=1}^{k_E} G_E^{e_s} \int_{e_s} x_i \, d\Sigma, \quad i = 1, \dots, d, \quad (3.4)$$

where  $(x_1, \dots, x_d)$  are the Cartesian coordinates.

We continue by pointing out the following identity:

$$\int_{\partial E} (\mathbb{K}\nabla x_i) \cdot \vec{n} x_j \, d\Sigma = \int_E \mathbb{K}\nabla x_i \cdot \nabla x_j \, dV = |E| \mathbb{K}_{ij}. \quad (3.5)$$

If we further introduce the  $k_E \times d$  matrices  $\mathbb{R}$  and  $\mathbb{N}$  by

$$\mathbb{R}_{s,i} = \int_{e_s} x_i \, d\Sigma \quad \text{and} \quad \mathbb{N}_{s,i} = (\mathbb{K}\nabla x_i) \cdot \vec{n}_E^{e_s}, \quad (3.6)$$

where  $s = 1, 2, \dots, k_E$  and  $i = 1, \dots, d$ , the identity (3.5) becomes

$$\mathbb{R}^T \mathbb{N} = |E| \mathbb{K}, \quad (3.7)$$

implying, among other things, that both matrices  $\mathbb{N}$  and  $\mathbb{R}$  have full rank  $d$ .

Inserting (3.1) into (3.4), and using (3.6), Assumption **(S2')** becomes

$$\mathbb{M}_E \mathbb{N} = \mathbb{R}. \quad (3.8)$$

We next show that  $\mathbb{M}_E$  can be written as a sum of two positive semidefinite matrices. We first notice that the matrix

$$\mathbb{M}_0 \equiv \frac{1}{|E|} \mathbb{R} \mathbb{K}^{-1} \mathbb{R}^T \quad (3.9)$$

satisfies (3.8). Indeed, from (3.7) and (3.8) we have

$$\mathbb{M}_0 \mathbb{N} = \frac{1}{|E|} \mathbb{R} \mathbb{K}^{-1} \mathbb{R}^T \mathbb{N} = \mathbb{R}.$$

Thus, we proved the following lemma.

**Lemma 3.1** *Let  $\mathbb{R}$  be given by (3.6). Then,  $\mathbb{M}_0$  defined by (3.9) satisfies (3.8).*

The matrix  $\mathbb{M}_0$  is obviously symmetric but only positive semidefinite. Therefore, Assumption **(S1)** does not hold. The following result shows how  $\mathbb{M}_0$  can be completed so as to meet the positive definiteness requirement.

**Theorem 3.2** *Let  $\mathbb{C}$  be a  $k_E \times (k_E - d)$  matrix whose  $k_E - d$  columns span the null space of the full rank matrix  $\mathbb{N}^T$ , so that  $\mathbb{N}^T \mathbb{C} = 0$ . Then, for every  $(k_E - d) \times (k_E - d)$  symmetric positive definite matrix  $\mathbb{U}$ , the following symmetric matrix*

$$\mathbb{M}_E = \mathbb{M}_0 + \mathbb{C} \mathbb{U} \mathbb{C}^T \quad (3.10)$$

*satisfies (3.8) and is positive definite.*

Proof. By construction,  $\mathbb{M}_E \mathbb{N} = \mathbb{M}_0 \mathbb{N}$ , and therefore by Lemma 3.1,  $\mathbb{M}_E$  satisfies (3.8). Moreover, still by construction,  $\mathbb{M}_E$  is symmetric and positive semidefinite. We are left to show that it is nonsingular. Let us assume that there exists a non-zero vector  $\mathbf{v}$  such that  $\mathbb{M}_E \mathbf{v} = 0$ . Then we must have,

$$\left\| \frac{1}{|E|^{1/2}} \mathbb{K}^{-1/2} \mathbb{R}^T \mathbf{v} \right\|^2 + \left\| \mathbb{U}^{1/2} \mathbb{C}^T \mathbf{v} \right\|^2 = 0 \quad (3.11)$$

which in turn implies that  $\mathbb{R}^T \mathbf{v} = 0$  and  $\mathbb{C}^T \mathbf{v} = 0$ . Hence  $(\mathbf{v}, \mathbb{C} \mathbf{u}) = 0$  for any vector  $\mathbf{u}$  in  $\mathfrak{R}^{k_E}$ , and therefore we get

$$\mathbf{v} \in \{\text{im}(\mathbb{C})\}^\perp = \{\ker(\mathbb{N}^T)\}^\perp = \text{im}(\mathbb{N}),$$

so that  $\mathbb{R}^T \mathbf{v} = \mathbb{R}^T \mathbb{N} \mathbf{w} = 0$  for some  $\mathbf{w} \in \mathfrak{R}^d$ . Now the identity (3.7) implies that  $\mathbf{w} = 0$ , so that  $\mathbf{v} = 0$ , and the nonsingularity of  $\mathbb{M}_E$  follows.  $\square$

Let us compute the dimension of the space of matrices  $\mathbb{M}_E$  having the form (3.10). Since  $\mathbb{U}$  has size  $k_E - d$ , a general symmetric positive definite matrix of this size has at least  $(k_E - d + 1)(k_E - d)/2$  free parameters. In the particular case of a triangular element, we get a 1-parameter family of matrices, which confirms the results of [13].

One of the efficient ways for solving the discrete problem (2.8) is based on the KKT theory of constrained minimization (see e.g. [16, Chapter 16]) where the constraints are given by (2.2). The solution of the KKT system is reduced to a solution of a sparse system for Lagrange multipliers with a symmetric positive definite matrix. This is what in the Finite Element context is often called *hybridization* and is usually attributed to Fraeijns de Veubeke [5] (see also [2], or [3] pag. 178–181). The procedure requires the inversion of  $\mathbb{M}_E$ . More precisely, during the whole procedure we *only* need the matrix  $\mathbb{M}_E^{-1}$ , while the explicit knowledge of the matrix  $\mathbb{M}_E$  is not required. In the following theorem we show that we can, in some sense, compute directly  $\mathbb{M}_E^{-1}$  *without computing*  $\mathbb{M}_E$ .

**Theorem 3.3** *Let  $\mathbb{D}$  be a  $k_E \times (k_E - d)$  matrix whose image spans the null space of  $\mathbb{R}^T$ , that is  $\text{im}(\mathbb{D}) = \ker(\mathbb{R}^T)$ , and let  $\tilde{\mathbb{U}}$  be an arbitrary symmetric positive definite  $(k_E - d) \times (k_E - d)$  matrix. Then the matrix*

$$\mathbb{W}_E := \frac{1}{|E|} \mathbb{N} \mathbb{K}^{-1} \mathbb{N}^T + \mathbb{D} \tilde{\mathbb{U}} \mathbb{D}^T \quad (3.12)$$

*is symmetric and positive definite and satisfies*

$$\mathbb{W}_E \mathbb{R} = \mathbb{N}. \quad (3.13)$$

The proof of this theorem follows the proofs of Lemma 3.1 and Theorem 3.2 and therefore it is omitted here. Note that the matrix  $\mathbb{N}$  contains the material properties and thus the first term in (3.12) is scaled properly.

Since, in practice, we are interested *only* in the matrix  $\mathbb{M}_E^{-1}$ , we could define  $\mathbb{M}_E^{-1} := \mathbb{W}_E$ . Indeed, the matrix  $\mathbb{M}_E$  defined this way will be symmetric positive definite and will satisfy (3.8). Moreover, it is not difficult to see that the matrix  $\mathbb{M}_E := \mathbb{W}_E^{-1}$  can still be written in the form (3.10), where the choice of the matrices  $\mathbb{U}$  and  $\mathbb{C}$  obviously depend on the choice of  $\tilde{\mathbb{U}}$  and  $\mathbb{D}$ .

**Remark 3.4** *The convergence estimates derived in [4] can be immediately applied here to get the first order convergence for both scalar and vector unknowns. Note that the numerical experiments in section 4 show pressure superconvergence for a variety of matrices  $\tilde{\mathbb{U}}$ . We shall investigate this superconvergence in future publications.*

### 3.1 Spectral analysis

Assumption **(S1)** imposes some restrictions on the choice of the *parameter* matrix  $\mathbb{U}$  in Theorem 3.2 (or on  $\tilde{\mathbb{U}}$  in Theorem 3.3), and requires fixing some further hypotheses on the shape-regularity of the mesh elements. In this paper, we use the conditions formulated initially in [4] for polyhedral meshes. They hold for basically all meshes which are not totally unreasonable, thus making our discretization methodology appealing in practical applications. For instance, they allow degenerate and non-convex elements (see, e.g. Fig. 1).

Let  $h_E$  denote a diameter of  $E$ . The set of shape-regularity assumptions is as follows.

- (M1) There exist two positive integers  $N_e$  and  $N_\ell$  such that every element  $E$  has at most  $N_e$  faces, and each face  $e$  has at most  $N_\ell$  edges.
- (M2) There exists a positive number  $\tau_*$  such that every element  $E$  is star-shaped with respect to every point of a sphere (a disk in 2D) with center at a point  $C_E \in E$  and radius  $\tau_* h_E$  (see Fig. 1).
- (M3) There exists a positive number  $\gamma_*$  such that each face  $e$  of element  $E$  is star-shaped with respect to every point of a disk of radius  $\gamma_* h_E$  centered at a point  $C_e \in e$ .
- (M4) For every element  $E$ , and for every face  $e$  of  $E$ , there exists a pyramid  $P_E^e$  contained in  $E$  such that its base is equal to  $e$ , its height is equal to  $\gamma_* h_E$  and the projection of its vertex onto  $e$  is  $C_e$ .

Before entering the discussion on Assumption **(S1)**, we rescale the matrices  $\mathbb{N}$  and  $\mathbb{R}$  and prove a technical lemma. Let us define

$$\tilde{\mathbb{N}} := \mathbb{N}\mathbb{K}^{-1} \quad \text{and} \quad \tilde{\mathbb{R}} := \frac{1}{|E|}\mathbb{R} \quad (3.14)$$

so that

$$\tilde{\mathbb{R}}^T \tilde{\mathbb{N}} = \tilde{\mathbb{N}}^T \tilde{\mathbb{R}} = \mathbb{I}. \quad (3.15)$$

Moreover, given a matrix  $\mathbb{N}$ ,  $\|\mathbb{N}\|$  denotes the matrix norm induced by the Euclidean vector norm, so that  $\|\mathbb{N}\| = \|\mathbb{N}^T\|$  holds. Then, we have the following lemma.

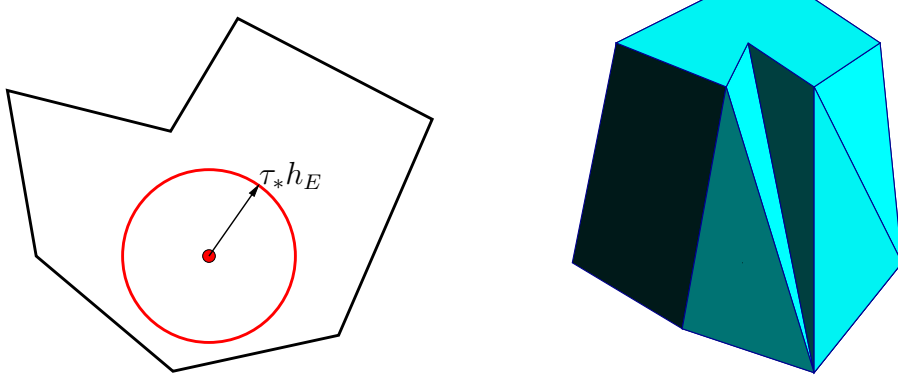


Figure 1: Examples of allowed elements in 2D and 3D.

**Lemma 3.5** *Assume that (M1) and (M2) hold. Then, we have the following upper bounds:*

$$\|\tilde{\mathbb{N}}\| \leq \sqrt{N_e}, \quad \|\tilde{\mathbb{R}}\| \leq \frac{d}{\tau_*}, \quad (3.16)$$

and the following lower bounds:

$$\|\tilde{\mathbb{R}}^T \mathbf{v}\| \geq \frac{1}{\sqrt{N_e}} \|\mathbf{v}\| \quad \forall \mathbf{v} \in \text{im}(\tilde{\mathbb{N}}) \quad (3.17)$$

and

$$\|\tilde{\mathbb{N}}^T \mathbf{v}\| \geq \frac{\tau_*}{d} \|\mathbf{v}\| \quad \forall \mathbf{v} \in \text{im}(\tilde{\mathbb{R}}). \quad (3.18)$$

Proof. We begin with the estimate on  $\tilde{\mathbb{N}}$ . For every  $\mathbf{w} \in \mathfrak{R}^d$ , we have

$$\|\tilde{\mathbb{N}}\mathbf{w}\|^2 = \sum_{s=1}^{k_E} \left( \sum_{i=1}^d n_i^{e_s} w_i \right)^2 \leq \|\mathbf{w}\|^2 \sum_{s=1}^{k_E} \sum_{i=1}^d (n_i^{e_s})^2 = \|\mathbf{w}\|^2 \sum_{s=1}^{k_E} 1 = N_e \|\mathbf{w}\|^2. \quad (3.19)$$

We now estimate the norm of  $\tilde{\mathbb{R}}$ . We denote by  $\mathbf{x}_{B_s}$  the barycenter of face  $e_s$ . Then, for every  $\mathbf{w} \in \mathfrak{R}^d$ , we have

$$|E|^2 \|\tilde{\mathbb{R}}\mathbf{w}\|^2 = \sum_{s=1}^{k_E} \left( \sum_{i=1}^d \int_{e_s} x_i d\Sigma w_i \right)^2 \leq \|\mathbf{w}\|^2 \sum_{s=1}^{k_E} \sum_{i=1}^d \left( \int_{e_s} x_i \right)^2 = \|\mathbf{w}\|^2 \sum_{s=1}^{k_E} |e_s|^2 |\mathbf{x}_{B_s}|^2 \quad (3.20)$$

Recall that we put the origin in the barycenter of  $E$ , so that  $|\mathbf{x}_{B_s}| \leq h_E$ . We consider now, for each face  $e_s$ , the pyramid  $P_s$  (triangle in 2D) having  $e_s$  as base, and the point  $C_E$  of Assumption (M2) as the vertex. This assumption implies that the height,  $h_s$ , of pyramid  $P_s$  is bigger than  $h_E \tau_*$ . As a consequence, we have

$$d|E| = d \sum_{s=1}^{k_E} |P_s| = \sum_{s=1}^{k_E} |e_s| h_s \geq h_E \tau_* \sum_{s=1}^{k_E} |e_s|.$$

This gives us the following estimate:

$$\sum_{s=1}^{k_E} |e_s|^2 |\mathbf{x}_{B_s}|^2 \leq h_E^2 \left( \sum_{s=1}^{k_E} |e_s| \right)^2 \leq \frac{d^2 |E|^2}{\tau_*^2}.$$

Inserting this in (3.20), we have

$$\|\tilde{\mathbb{R}}\mathbf{w}\|^2 \leq \|\mathbf{w}\|^2 \frac{d^2}{\tau_*^2}. \quad (3.21)$$

The proofs of (3.17) and (3.18) follow almost immediately: let us show the first one. For every  $\mathbf{v} \in \text{im}(\tilde{\mathbb{N}})$  we have  $\mathbf{v} = \tilde{\mathbb{N}}\mathbf{w}$  for some  $\mathbf{w} \in \mathfrak{R}^d$ . Hence, from (3.15) and (3.16) we have

$$\|\tilde{\mathbb{R}}^T \mathbf{v}\|^2 = \|\tilde{\mathbb{R}}^T \tilde{\mathbb{N}}\mathbf{w}\|^2 = \|\mathbf{w}\|^2 \geq \frac{1}{N_e} \|\tilde{\mathbb{N}}\mathbf{w}\|^2 = \frac{1}{N_e} \|\mathbf{v}\|^2.$$

The proof of (3.18) is identical.  $\square$

From Lemma 3.5 we may easily obtain estimates for the *unscaled* matrices  $\mathbb{R}$  and  $\mathbb{N}$  and their products with the tensor  $\mathbb{K}$ . In particular, we may prove that

$$\|\mathbb{K}^{-1/2} \mathbb{R}^T \mathbf{v}\|^2 \leq \frac{d^2 |E|^2}{\kappa_* \tau_*^2} \|\mathbf{v}\|^2 \quad (3.22)$$

and

$$\|\mathbf{v}\|^2 \leq \frac{N_e \kappa_*}{|E|^2} \|\mathbb{K}^{-1/2} \mathbb{R}^T \mathbf{v}\|^2 \quad \forall \mathbf{v} \in \text{im}(\mathbb{N}). \quad (3.23)$$

It is obvious that the matrix  $\mathbb{M}_E$  will satisfy Assumption **(S1)** *if and only if* its inverse matrix satisfies it. Hence, in what follows, we discuss only the case of the matrix  $\mathbb{M}_E$ . If one decides to follow the path of Theorem 3.3 (constructing directly the matrix  $\mathbb{W}_E = \mathbb{M}_E^{-1}$ ), the same arguments will hold for  $\mathbb{W}_E$  as well.

**Theorem 3.6** *Let the assumptions of Theorem 3.2 and Lemma 3.5 hold. Assume further that there exist two positive constants  $s_U^*$  and  $S_U^*$ , independent of  $E$ , such that*

$$s_U^* |E| \|\mathbf{v}\|^2 \leq \|\mathbb{U}^{1/2} \mathbb{C}^T \mathbf{v}\|^2 \quad \forall \mathbf{v} \in \text{im}(\mathbb{C}) \quad (3.24)$$

and

$$\|\mathbb{U}^{1/2} \mathbb{C}^T \mathbf{v}\|^2 \leq S_U^* |E| \|\mathbf{v}\|^2 \quad \forall \mathbf{v} \in \mathfrak{R}^{k_E - d}. \quad (3.25)$$

*Then, the matrix  $\mathbb{M}_E$  constructed as in (3.10) satisfies Assumption **(S1)**. In particular, we have*

$$\min \left\{ \frac{1}{2} s_U^*, \sigma_* \right\} |E| \|\mathbf{v}\|^2 \leq \|\mathbb{M}_E^{1/2} \mathbf{v}\|^2 \leq \max \{ S_U^*, \sigma^* \} |E| \|\mathbf{v}\|^2 \quad \forall \mathbf{v} \in \mathfrak{R}^{k_E} \quad (3.26)$$

where

$$\sigma_* = \frac{\kappa_* \tau_*^2 s_U^*}{N_e \kappa_* (2d^2 + s_U^* \kappa_* \tau_*^2)} \quad \text{and} \quad \sigma^* = \frac{d^2}{\kappa_* \tau_*^2}.$$

Proof. We have  $\|\mathbb{M}_E^{1/2}\mathbf{v}\|^2 = \|\mathbb{M}_0^{1/2}\mathbf{v}\|^2 + \|\mathbb{U}^{1/2}\mathbb{C}^T\mathbf{v}\|^2$ . The upper bound follows from (3.22),

$$\|\mathbb{M}_0^{1/2}\mathbf{v}\|^2 = \frac{1}{|E|} \|\mathbb{K}^{-1/2}\mathbb{R}^T\mathbf{v}\|^2 \leq \frac{d^2|E|}{\kappa_*\tau_*^2} \|\mathbf{v}\|^2, \quad (3.27)$$

and (3.25). The lower bound is obtained as follows. The definition of the matrix  $\mathbb{C}$  implies that

$$\mathfrak{R}^{k_E} \equiv \text{im}(\mathbb{N}) \oplus \{\text{im}(\mathbb{N})\}^\perp \equiv \text{im}(\mathbb{N}) \oplus \ker(\mathbb{N}^T) = \text{im}(\mathbb{N}) \oplus \text{im}(\mathbb{C})$$

and, therefore, any vector  $\mathbf{v} \in \mathfrak{R}^{k_E}$  can be uniquely written as  $\mathbf{v} = \mathbf{v}_N + \mathbf{v}_C$  where  $\mathbf{v}_N \in \text{im}(\mathbb{N})$  and  $\mathbf{v}_C \in \text{im}(\mathbb{C})$ . Moreover,  $\|\mathbf{v}\|^2 = \|\mathbf{v}_N\|^2 + \|\mathbf{v}_C\|^2$ . We also recall that there are two constants  $\alpha$  and  $\beta$  independent of  $h$  such that

$$\|\mathbb{K}^{-1/2}\mathbb{R}^T\mathbf{v}_N\|^2 \geq \alpha|E|^2\|\mathbf{v}_N\|^2 \quad \text{and} \quad \|\mathbb{K}^{-1/2}\mathbb{R}^T\mathbf{v}_C\|^2 \leq \beta|E|^2\|\mathbf{v}_C\|^2. \quad (3.28)$$

In particular the first estimate follows from (3.23) with  $\alpha = (N_e\kappa_*)^{-1}$ , and the second follows from (3.22) with  $\beta = d^2(\tau_*^2\kappa_*)^{-1}$ . Now, we use the following inequality,

$$-2\mathbf{a} \cdot \mathbf{c} \leq \varepsilon\|\mathbf{a}\|^2 + \frac{1}{\varepsilon}\|\mathbf{c}\|^2, \quad \forall \varepsilon > 0,$$

to get

$$\begin{aligned} \|\mathbb{M}_E^{1/2}\mathbf{v}\|^2 &= \frac{1}{|E|} \|\mathbb{K}^{-1/2}\mathbb{R}^T\mathbf{v}\|^2 + \|\mathbb{U}^{1/2}\mathbb{C}^T\mathbf{v}\|^2 \\ &\geq \frac{1}{|E|} \|\mathbb{K}^{-1/2}\mathbb{R}^T(\mathbf{v}_N + \mathbf{v}_C)\|^2 + s_U^*|E| \|\mathbf{v}_C\|^2 \\ &\geq \frac{1}{|E|} \|\mathbb{K}^{-1/2}\mathbb{R}^T\mathbf{v}_N\|^2(1 - \varepsilon) + \frac{1}{|E|} \|\mathbb{K}^{-1/2}\mathbb{R}^T\mathbf{v}_C\|^2 \left(1 - \frac{1}{\varepsilon}\right) + s_U^*|E| \|\mathbf{v}_C\|^2. \end{aligned}$$

If we take  $\varepsilon < 1$  and apply inequalities (3.28), we get the following estimate:

$$\|\mathbb{M}_E^{1/2}\mathbf{v}\|^2 \geq (1 - \varepsilon)\alpha|E| \|\mathbf{v}_N\|^2 + \left(1 - \frac{1}{\varepsilon}\right)\beta + s_U^* \Big|E\| \|\mathbf{v}_C\|^2.$$

The lower bound follows for  $\varepsilon = \beta/(\beta + \frac{1}{2}s_U^*)$ .  $\square$

In actual numerical computations (based on Theorem 3.2), we recommend to multiply the matrix  $\mathbb{U}$  by a characteristics value of  $\mathbb{K}^{-1}$  over the element  $E$ , for example, its trace. This will improve the spectral properties of the matrix  $\mathbb{M}_E$  with respect to material properties. The estimates in (3.26) provide an illustration of the practical role of  $\mathbb{U}$  in the conditioning of  $\mathbb{M}_E$ . As long as the extreme eigenvalues of  $\mathbb{U}$  are within those of  $\mathbb{K}^{-1}$ , the conditioning of  $\mathbb{M}_E$  is not strongly affected by the choice of  $\mathbb{U}$ . The same remark obviously applies to the matrix  $\tilde{\mathbb{U}}$ , if we decide to use Theorem 3.3 to construct directly the matrix  $\mathbb{M}_E^{-1}$ . This latter approach is what we have employed in our experiments.

## 3.2 Computational considerations

According to Theorem 3.3, the most computationally demanding part in building  $\mathbb{M}_E^{-1} = \mathbb{W}_E$  is the construction of the matrix  $\mathbb{D}$ . We recommend two algorithms. The first one is based on the LAPACK routine *dgesvd* which computes the right singular vectors of  $\mathbb{R}^T$ . The cost of obtaining these vectors for a matrix of size  $k_E \times d$ , is about  $4k_E d^2 + 8k_E^3$  (see e.g. [7]). The second algorithm is much cheaper, and it may be used, for instance, when  $\tilde{\mathbb{U}}$  is selected as  $\tilde{\mathbb{U}} = \tilde{u}\mathbb{I}$ , with  $\tilde{u} > 0$ . In this case, we can write  $\mathbb{D}\tilde{\mathbb{U}}\mathbb{D}^T = \tilde{u}\mathbb{D}\mathbb{D}^T =: \tilde{u}\tilde{\mathbb{D}}$ , and  $\tilde{\mathbb{D}}$  can be computed without explicitly constructing  $\mathbb{D}$ . Let us assume that the matrix  $\mathbb{R}$  is given.

**Algorithm 1** (*Construction of matrix  $\mathbb{W}_E$* )

1. Orthonormalize columns of the matrix  $\mathbb{R}$  using the Gauss-Schmidt algorithm. Let  $\tilde{\mathbb{R}}$  be the resulting matrix,  $\tilde{\mathbb{R}} = [\tilde{\mathbf{r}}_1, \dots, \tilde{\mathbf{r}}_d]$ .
2. For  $s = 1, 2, \dots, k_E$  do
  - (a) Take a vector  $\mathbf{e}_s$  with all zero entries except one at position  $s$ .
  - (b) Orthogonalize this vector with respect to the columns of  $\tilde{\mathbb{R}}$ :

$$\tilde{\mathbf{d}}_s := \mathbf{e}_s - \sum_{i=1}^d \tilde{r}_{i,s} \tilde{\mathbf{r}}_i$$

where  $\tilde{r}_{s,i}$  is the  $s$ -th component of the vector  $\tilde{\mathbf{r}}_i$ .

- (c) Make vector  $\tilde{\mathbf{d}}_s$  the  $s$ -th column of matrix  $\tilde{\mathbb{D}}$ .

3. Build the matrix  $\mathbb{W}_E$  as follows:

$$\mathbb{W}_E = \frac{1}{|E|} \mathbb{N} \mathbb{K}^{-1} \mathbb{N}^T + \tilde{u} \tilde{\mathbb{D}} \equiv \frac{1}{|E|} \tilde{\mathbb{N}} \mathbb{K} \tilde{\mathbb{N}}^T + \tilde{u} \tilde{\mathbb{D}}.$$

It is pertinent to note that the matrix  $\tilde{\mathbb{D}}$  built in Algorithm 1 is a square  $k_E \times k_E$  matrix having only  $k_E - d$  linearly independent columns. Thus, the matrix  $\mathbb{D}$  in  $\tilde{\mathbb{D}} = \mathbb{D}\mathbb{D}^T$  has full column rank equal to  $(k_E - d)$ . In matrix form we have  $\tilde{\mathbb{D}} = \mathbb{I} - \tilde{\mathbb{R}}\tilde{\mathbb{R}}^T$ , i.e.  $\tilde{\mathbb{D}}$  is symmetric and is the orthogonal projector ( $\tilde{\mathbb{D}} = \tilde{\mathbb{D}}^2$ ) onto the space  $\{\text{im}(\mathbb{R})\}^\perp$ .

Let us compare the computational complexity of our method with the method proposed in [10, 12]. We assume that  $\mathbb{K}$  is a full tensor, that  $\tilde{\mathbb{U}}$  is a multiple of the identity matrix,  $\tilde{\mathbb{U}} = \tilde{u}\mathbb{I}$ ,  $\tilde{u} > 0$ , and that all geometric objects (normals, areas, volumes, etc.) are already known. The second step in Algorithm 1 requires  $d k_E^2 + O(k_E)$  flops. Therefore, the complexity of building the matrix  $\mathbb{W}_E$  is equal to

$$(2d + 1) k_E^2 + 4d^2 k_E \text{ flops.}$$

The method in [10] requires a partition of element  $E$  onto simplicial elements (which by itself is already a non-trivial task for non-convex elements). Let us denote the number of

interior (partition) faces (edges in 2D) by  $p_E$ , and the number of simplicial elements by  $t_E$ . Then, omitting the quadratic terms, the most efficient implementation of their method requires

$$\frac{4}{3}(k_E^3 + p_E^3 + t_E^3) + p_E k_E (2p_E + k_E + 2t_E)$$

flops to build the matrix  $\mathbb{W}_E = \mathbb{M}_E^{-1}$ . The first three terms estimate the cost of inversion of symmetric positive definite matrices [7]. The other terms are the cost of a few matrix-matrix products. For polygonal meshes and partitions using a center point, we have  $k_E = p_E = t_E$  and therefore the complexity is  $9k_E^3 + O(k_E^2)$ . The same argument can be used to estimate the complexity for a hexahedron when it is split into 6 tetrahedra. For a minimal partition of the hexahedron using a central point, we get  $p_E = 3k_E$ ,  $t_E = 2k_E$ , and the complexity rockets up to  $81k_E^3 + O(k_E^2)$ .

## 4 Numerical experiments

Remark 3.4 implies that the main focus of numerical experiments should be on superconvergence of the scalar variable. For this reason, we consider a variety of arbitrary matrices  $\tilde{\mathbb{U}}$  satisfying the conditions of Theorem 3.6. We also consider diffusion problems with sufficiently smooth solutions, so that we may expect the second order convergence rate for the scalar variable  $\mathbf{p}_h$  and the first order convergence rate for the other primary variable  $\mathbf{F}_h$  on unstructured polygonal and polyhedral meshes.

We shall measure the accuracy of the discrete solution  $(\mathbf{p}_h, \mathbf{F}_h)$  in the *natural* norms induced by the scalar products (2.3) and (2.4). Let  $(\mathbf{p}^I, \mathbf{F}^I)$  be the interpolated solution where  $\mathbf{p}^I$  is the vector of mean values of the solution  $p$  over the elements and  $\mathbf{F}^I$  is given by (3.1). We define the following discrete  $L_2$  errors:

$$|||\mathbf{p}^I - \mathbf{p}_h||| = [\mathbf{p}^I - \mathbf{p}_h, \mathbf{p}^I - \mathbf{p}_h]_Q^{1/2}, \quad |||\mathbf{F}^I - \mathbf{F}_h||| = [\mathbf{F}^I - \mathbf{F}_h, \mathbf{F}^I - \mathbf{F}_h]_X^{1/2}.$$

We also present errors in the maximum norm in the Euclidean space that we shall denote by  $||| \cdot |||_\infty$ .

For all meshes considered in this section, we have performed the following consistency check. We have solved the Dirichlet boundary value problem with a constant tensor  $\mathbb{K}$  and an exact solution  $p^1$  given by  $p^1 = x_1 + \dots + x_d$ . As  $p^1$  is linear, it follows from Assumption **(S2)** that the errors should be zero, and this is indeed observed in our experiments.

In most experiments the diffusion tensor is a function of the space coordinates. Therefore, to compute the elemental matrices  $\mathbb{M}_E$  we evaluated the tensor  $\mathbb{K}$  at the center of mass of each element. For every element  $E$ , we denote by  $\mathbb{K}_E$  the corresponding value.

The discrete problem (for the Lagrange multipliers) was solved with the preconditioned conjugate gradient (PCG) method. A V-cycle of the algebraic multigrid [17] was chosen as the preconditioner. The stopping criterion for the PCG method was a reduction of the Euclidean norm of the residual by a factor  $10^{-12}$ .

**Example 1.** We consider the Dirichlet boundary value problem (1.1) in the unit square  $[0, 1]^2$  with the exact solution (see also the right picture in Fig. 2)

$$p(x, y) = x^3 y^2 + x \sin(2\pi xy) \sin(2\pi y).$$

The diffusion tensor is taken as:

$$\mathbb{K} = \begin{pmatrix} (x+1)^2 + y^2 & -xy \\ -xy & (x+1)^2 \end{pmatrix}.$$

We consider a sequence of polygonal median meshes built as follows. First, we define a set of points  $\mathbf{x}_{i,j} = (x_{1,i,j}, x_{2,i,j})$  for generating the Voronoi tessellation:

$$\begin{aligned} x_{1,i,j} &= \xi_i + 0.1 \sin(2\pi\xi_i) \sin(2\pi\eta_j), & i &= 0, \dots, n, \\ x_{2,i,j} &= \eta_j + 0.1 \sin(2\pi\xi_i) \sin(2\pi\eta_j), & j &= 0, \dots, n, \end{aligned}$$

where  $\xi_i = ih$ ,  $\eta_j = jh$  and  $h = 1/n$ . Then, a median mesh (see Fig. 2) is constructed from the Voronoi mesh by moving a mesh vertex to the center of mass of a triangle formed by the centers of three Voronoi cells sharing the vertex.

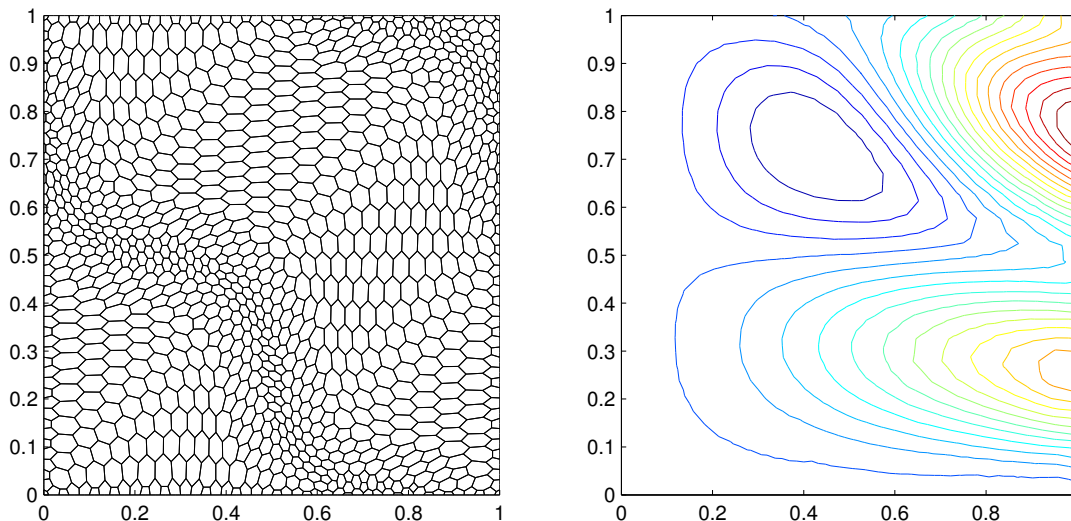


Figure 2: Polygonal mesh and solution isolines for example 1.

For every element  $E$ , we define a scalar matrix  $\tilde{\mathbb{U}} = \tilde{u}_E \mathbb{I}$  where  $\tilde{u}_E = \text{trace}(\mathbb{K}_E)/|E|$ . The result of our numerical experiments are collected in Table 1. Global convergence rates were computed using linear regression analysis. We observe superconvergence of both variables in the natural norms. Note that a convergence rate of 1.5 for the flux variable is typical for the Dirichlet boundary value problem and is observed in other lower order discretization schemes on smooth triangular and quadrilateral meshes (see e.g. [1] and references therein).

As shown in Theorem 3.6, the spectral properties of the matrix  $\mathbb{M}_E$  (and of  $\mathbb{W}_E$ ) depend on a balance between the extreme eigenvalues of  $\mathbb{K}$  and  $\mathbb{U}$ . In this paper, we investigate this dependence only for a matrix  $\tilde{\mathbb{U}}$  in  $\mathbb{W}_E$  in the form  $\tilde{\mathbb{U}} = \tilde{u} \mathbb{I}$  where  $\tilde{u} > 0$ . Fig 3 shows errors (vertical axis) as functions of  $\tilde{u}/\tilde{u}_E$  (horizontal axis) for the case  $1/h = 32$ . There is a quite big interval  $\tilde{u} \in [2, 80]$  where the errors vary only 3 times. What is remarkable here is that for all values of  $\tilde{u}$  we observed second order convergence rate for  $\mathbf{p}_h$  and 1.5 convergence rate for  $\mathbf{F}_h$ .

Table 1: Convergence analysis on polygonal meshes.

$1/h$	$    \mathbf{p}^I - \mathbf{p}_h    $	$    \mathbf{F}^I - \mathbf{F}_h    $	$    \mathbf{p}^I - \mathbf{p}_h    _\infty$	$    \mathbf{F}^I - \mathbf{F}_h    _\infty$
16	5.17e-2	7.38e-1	1.61e-1	5.25e-0
32	1.18e-2	2.44e-1	4.54e-2	2.80e-0
64	2.76e-3	8.45e-2	1.28e-2	1.46e-0
128	6.65e-4	2.89e-2	3.06e-3	7.79e-1
rate	2.09	1.56	1.90	0.92

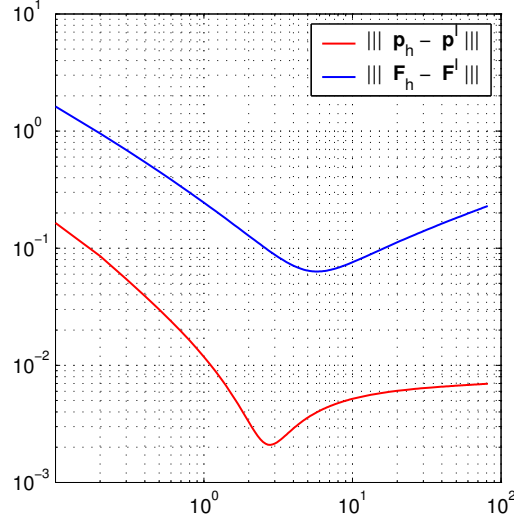


Figure 3: Errors as function of  $\tilde{u}/\tilde{u}_E$  in example 1.

**Example 2.** We consider the Dirichlet boundary value problem (1.1) in the unit square  $[0, 1]^2$ . Let the diffusion tensor  $\mathbb{K}$  be scalar and equal to  $K_1\mathbb{I}$  in the region defined by  $y < 0.5$  and  $K_2\mathbb{I}$  in the rest of the domain. The source term is chosen in such a way that the exact solution is

$$p(x, y) = \begin{cases} a + bx + cy^m, & y < 0.5, \\ a + c \frac{K_2 - K_1}{2^m K_2} + bx + c \frac{K_1}{K_2} y^m, & y \geq 0.5. \end{cases} \quad (4.1)$$

We consider a sequence of non-matching meshes as shown in Fig. 4. The random grids below and above the interface line  $y = 0.5$  were generated by moving each mesh point  $P$  (of an originally uniform mesh) to a random position inside a square  $S(P)$  centered at the point. The sides of  $S(P)$  were aligned with the coordinate axes and their length was equal to 80% of the size of the smallest edge (in the original uniform grid) having  $P$  as an endpoint.

In our method, we treat a non-matching mesh as a conformal polygonal mesh. When

Table 2: Convergence analysis on non-matching meshes.

#cells	$\ \mathbf{p}^I - \mathbf{p}_h\ $	$\ \mathbf{F}^I - \mathbf{F}_h\ $	$\ \mathbf{p}^I - \mathbf{p}_h\ _\infty$	$\ \mathbf{F}^I - \mathbf{F}_h\ _\infty$
780	1.01e-2	1.12e-1	2.82e-2	7.80e-1
3286	2.36e-3	4.72e-2	6.70e-3	3.51e-1
13482	5.73e-4	2.24e-2	1.78e-3	1.38e-1
54610	1.41e-4	1.09e-2	4.37e-4	7.70e-2
rate	2.01	1.09	1.95	1.11

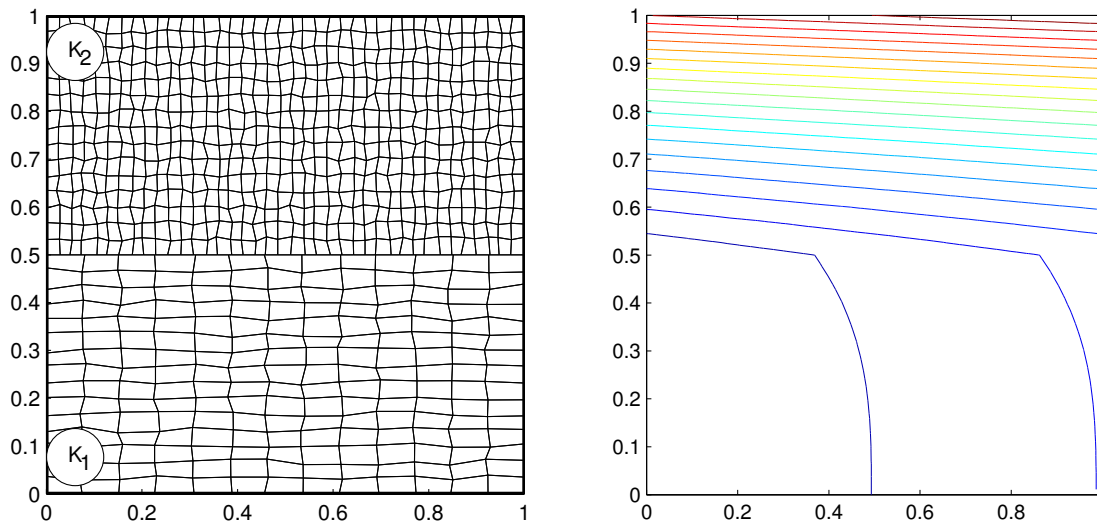


Figure 4: Polygonal mesh and solution isolines for example 2.

$m = 1$  in (4.1), the exact solution is linear, and both errors are equal to zero for all values of the other parameters, i.e. the discretization scheme is exact for piecewise linear solutions.

In the following numerical experiments we use  $a = b = c = 1$ ,  $K_1 = 10$ ,  $K_2 = 1$  and  $m = 3$ . See Table 2. We observe superconvergence of the scalar variable in both norms. The lack of flux superconvergence is typical for random meshes and is observed in other similar discretization schemes on simplicial meshes.

**Example 3.** Let us consider the Dirichlet boundary value problem (1.1) with the exact solution

$$p(x, y) = x^3 y^2 z + x \sin(2\pi xy) \sin(2\pi yz) \sin(2\pi z).$$

We take the diffusion tensor as:

$$\mathbb{K} = \begin{pmatrix} 1 + y^2 + z^2 & -xy & -xz \\ -xy & 1 + x^2 + z^2 & -yz \\ -xz & -yz & 1 + x^2 + y^2 \end{pmatrix}.$$

It is not difficult to check that  $\mathbb{K}$  is a positive definite matrix for all values of  $x$ ,  $y$  and  $z$ .

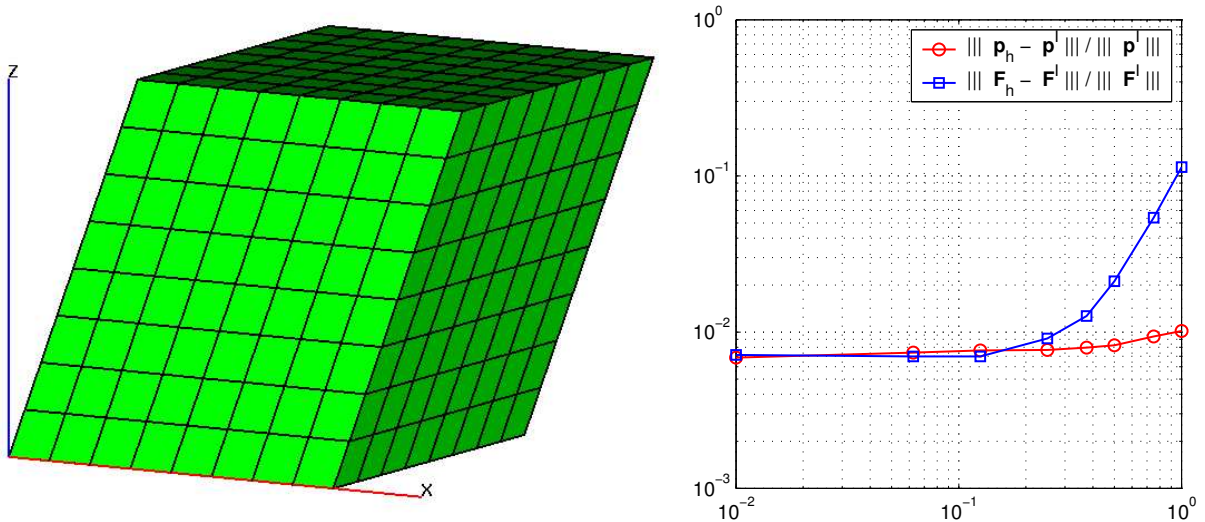


Figure 5: Polyhedral mesh for Example 3 corresponding to  $\varepsilon = 0.25$  (left) and the relative errors as functions of  $\varepsilon$  (right).

We consider a sequence of uniform cubic meshes in the unit cube  $[0, 1]^3$  and generate a corresponding sequence of hexahedral meshes using the following linear transformation:

$$\tilde{x} = x + \varepsilon z, \quad \tilde{y} = y + \varepsilon z, \quad \tilde{z} = z.$$

An example of a modified mesh is shown in Fig. 5: it corresponds to  $\varepsilon = 0.25$  and  $h = 1/8$ , where  $h$  is the size of a cubic element in the original mesh. The results of numerical experiments presented in Table 3 show the superconvergence of the scalar variable in both norms and the superconvergence of the vector variable in the discrete  $L_2$ -norm.

Now, we fix the mesh topology by taking  $h = 1/32$  and vary the transformation parameter  $\varepsilon$ . The behavior of the relative errors is shown in Fig. 5. As expected, the errors grow when we increase  $\varepsilon$ . The unexpected result is that the error in the vector variable is more sensitive to the mesh deformation than the error in the scalar variable. For the case  $\varepsilon = 1.0$ , the method from [10, 12] gives a 75% smaller error in the scalar variable but a 83% bigger error in the vector variable. This indicates that further evidence is required to get more insight into the accuracy of different discretization methods. For example, for hexahedral meshes, comparisons with the mixed finite element method could be performed. We shall address this problem in future publications.

## Conclusion

We gave a rigorous mathematical description of a family of mimetic finite difference (MFD) discretizations for diffusion problems on unstructured polygonal and polyhedral meshes. It was shown in [4] that the convergence analysis of a MFD method is reduced to the existence of a solution of a matrix algebraic equation with constraints. In this paper, we developed

Table 3: Convergence analysis on polyhedral meshes.

$1/h$	$   \mathbf{p}^I - \mathbf{p}_h   $	$   \mathbf{F}^I - \mathbf{F}_h   $	$   \mathbf{p}^I - \mathbf{p}_h   _\infty$	$   \mathbf{F}^I - \mathbf{F}_h   _\infty$
8	3.83e-2	5.35e-1	1.55e-1	6.07e-0
16	1.10e-2	1.43e-1	4.83e-2	2.48e-0
32	2.86e-3	3.58e-2	1.26e-2	1.11e-0
64	7.21e-4	8.94e-3	3.28e-3	5.42e-1
rate	1.91	1.97	1.86	1.16

a computationally cheap solution method for this equation. With this new method, discretizations on polyhedral meshes look as simple as discretizations on tetrahedral meshes. The resulting MFD methods have optimal convergence rates for a wide variety of problems, including hanging nodes, distorted meshes and the presence of a full material tensor.

## Acknowledgments

The work was partly performed at the Los Alamos National Laboratory operated by the University of California for the US Department of Energy under contract W-7405-ENG-36. The second author acknowledges the partial support of the DOE/ASCR Program in the Applied Mathematical Sciences.

The authors thank Dr. R.Loubere (LANL) for his assistance in generating polygonal meshes and D. R.Garimella (LANL) for his help in using the mesh package MSTK [6].

## References

- [1] T. Arbogast, C. N. Dawson, P. T. Keenan, M. F. Wheeler, and I. Yotov. Enhanced cell-centered finite differences for elliptic equations on general geometry. *SIAM J. Sci. Comp.*, 19(2):404–425, 1998.
- [2] D.N. Arnold and F. Brezzi. Mixed and non-conforming finite element methods: implementation, post-processing and error estimates. *Math. Modelling Numer. Anal.*, 19:7–35, 1985.
- [3] F. Brezzi and M. Fortin. *Mixed and hybrid finite element methods*. Springer-Verlag, New York, 1991.
- [4] F. Brezzi, K. Lipnikov, and M. Shashkov. Convergence of mimetic finite difference method for diffusion problems on polyhedral meshes. *SIAM J. Numer. Anal.*, 2004. to appear.
- [5] B. Fraeijns de Veubeke. Displacement and equilibrium models in the finite element method. In O.C. Zienkiewicz and G. Holister, editors, *Stress Analysis*. John Wiley and Sons, New York, 1965.

- [6] R. Garimella. MSTK: A flexible infrastructure library for developing mesh-based applications. In *Proceedings of the 13th International Meshing Roundtable*, volume II, pages 1196–1204, 2004. <http://math.lanl.gov/~rao/Meshing-Projects/MSTK/>.
- [7] G. Golub and C. Van Loan. *Matrix Computations*. The Johns Hopkins University Press, Baltimore and London, 3rd Edition, 1996.
- [8] J. Hyman and M. Shashkov. The approximation of boundary conditions for mimetic finite difference methods. *Computers and Mathematics with Applications*, 36:79–99, 1998.
- [9] J. Hyman, M. Shashkov, and S. Steinberg. The numerical solution of diffusion problems in strongly heterogeneous non-isotropic materials. *J. Comput. Phys.*, 132:130–148, 1997.
- [10] Y. Kuznetsov, K. Lipnikov, and M. Shashkov. Mimetic finite difference method on polygonal meshes for diffusion-type problems. *Comp. Geosciences*, 2004. in press.
- [11] K. Lipnikov, J. Morel, and M. Shashkov. Mimetic finite difference methods for diffusion equations on non-orthogonal non-conformal meshes. *J. Comput. Phys.*, (in press), 2004.
- [12] K. Lipnikov, M. Shashkov, and D. Svyatskiy. The mimetic finite difference discretization of diffusion problem on unstructured polyhedral meshes. Technical Report LAUR-04-6310, Los Alamos National Laboratory, 2004. submitted to *J. Comp. Phys.*
- [13] R. Liska, M. Shashkov, and V. Ganza. Analysis and optimization of inner products for mimetic finite difference methods on triangular grid. *Mathematics and Computers in Simulation*, 67:55–66, 2004.
- [14] J. Morel, M. Hall, and M. Shashkov. A local support-operators diffusion discretization scheme for hexahedral meshes. *J. Comput. Phys.*, 170:338–372, 2001.
- [15] J. Morel, R. Roberts, and M. Shashkov. A local support-operators diffusion discretization scheme for quadrilateral  $r - z$  meshes. *J. Comput. Phys.*, 144:17–51, 1998.
- [16] J. Nocedal and Wright. *S. Numerical Optimization*. Springer-Verlag, New-York, Berlin, Heidelberg, 2000.
- [17] K. Stüben. Algebraic multigrid (AMG): experiences and comparisons. *Appl. Math. Comput.*, 13:419–452, 1983.